J. Chem. Thermodynamics 131 (2019) 303–313

Contents lists available at ScienceDirect

J. Chem. Thermodynamics

journal homepage: www.elsevier.com/locate/jct

Influence of temperature and pressure on the density and speed of sound of *N*-ethyl-2-hydroxyethylammonium propionate ionic liquid

João A. Sarabando [a], Paulo J.M. Magano [b], Abel G.M. Ferreira [a,*], Jaime B. Santos [b], Pedro J. Carvalho [c], Silvana Mattedi [d], Isabel M.A. Fonseca [a], Mário Santos [b]

[a] GERST – Group on Environment, Reaction, Separation and Thermodynamics, Department of Chemical Engineering, University of Coimbra, Rua Sílvio Lima, 3030-790 Coimbra, Portugal
[b] CEMMPRE, Department of Electrical and Computers Engineering, University of Coimbra, Polo II, Rua Sílvio Lima, 3030-970 Coimbra, Portugal
[c] CICECO –Aveiro Institute of Materials, Department of Chemistry, University of Aveiro, 3810-193 Aveiro, Portugal
[d] Escola Politécnica, Universidade Federal da Bahia, Rua Aristides Novis 2, Federação, 40210-630 Salvador, Bahia, Brazil

ARTICLE INFO

Article history:
Received 1 July 2018
Received in revised form 3 November 2018
Accepted 6 November 2018
Available online 17 November 2018

Keywords:
N-ethyl-2-hydroxyethylammonium propionate
Density
Speed of sound
GMA equation of state
Sun equation

ABSTRACT

The alkanolammonium ILs are protic ionic liquids (PILs) with low cost of preparation, simple synthesis and purification methodologies and low toxicity. The knowledge of high-pressure density and speed of sound are fundamental properties either to understand the nature of molecular interactions, structure and packing effects or to determine other thermodynamic properties useful in chemical and industrial processes. Herein, the density, up to 35 MPa along isotherms ranging from (298.15 to 343.15) K, and the speed of sound up to 20 MPa, along isotherms in the range (303.15 to 353.15) K, are reported for the *N*-ethyl-2-hydroxyethylammonium propionate, [E2HEA][Pr] PIL. The experimental *pVT* data were further correlated with the Goharshadi–Morsali–Abbaspour equation of state (GMA EoS) with average absolute deviation (*%AARD*) of 0.03%. From GMA EoS the thermal expansivity and isothermal compressibility were determined. The speed of sound was correlated with Sun equation with *%AARD* = 0.08%. The isentropic and molar compressibilities were also calculated from the density and speed of sound.

1. Introduction

The alkanolammonium ILs are protic ionic liquids (PILs) chemically characterized by presence of at least a proton which is/are able to promote extensive hydrogen bonding [1]. PILs have a broad range of applications which include biological and pharmaceuticals purposes [2–4], in organic synthesis [5], biodiesel production [6], electrolytes for polymer membrane fuel cells [7], cleaning [8], and as propellant or explosives [9].

The simple synthesis and purification processes [10,11] with associated low cost and toxicity compared with other ILs [12,13] are important points that justify their increasing use to which is associated a very important need for the knowledge of thermodynamic properties closely related with the applications. In this sense, a careful analysis of the literature leaves the impression that many more experimental determinations of the thermophysical properties of the alkanolammoniums are necessary for the development of successful correlations directed to the correct design of the production equipment and on the other hand for the development in the theoretical field. With regard to density, the studies can be summarized as follows. Kurnia et al. [10] made measurements at atmospheric pressure for hydroxyethylammonium and bis-(hydroxyethyl)ammonium cations with acetate and lactate anions. For hydroxyethylammonium propionate data were reported by Kurnia et al. [14] and recently, by us up to 35 MPa and at T = (298.15–343.15) K [15]. Alvarez et al. [16] reported density data for the N-methyl-2-hydroxyethylammonium cation with various carboxylates (formate, acetate, propionate, butyrate, isobutyrate and pentanoate). Pinkert et al. [17], presented density data for the 2-hydroxyethylammonium, 3-hydroxypropylammonium, bis(2-hydroxyethyl)ammonium, and tris(2-hydroxyethyl)ammonium cations combined with formate, acetate and malonate anions.

The experimental data available for the speed of sound of alkanolammonium PILs are very scarce as can be concluded by the data available in the NIST ILThermo database [18]. Experimental data of a total of 242 ILs, reported since 2010, is available for imidazolium (51%), pyridinium (16%), pyrrolidinium (9%), phosphonium (2%) and ammonium (23%), with hydroxyethylammoniums contributing only by 5%. The speed of sound has been reported for the methylhydroxyethylammonium [16] and 2-hydroxyethylammonium with carboxylate anions by Iglesias and coworkers

* Corresponding author.
E-mail address: abel@eq.uc.pt (A.G.M. Ferreira).

https://doi.org/10.1016/j.jct.2018.11.005
0021-9614/

[11,19,20]. Recently, the authors reported measurements up to 20 MPa in the range T = (303.15–353.15) K for 2-hydroxyethylammonium propionate [15].

This paper, which is a part of a wider project [21–23] aiming at measuring and correlate density and speed of sound of PILs and their aqueous mixtures, presents density and speed of sound measurements for the *N*-ethyl-2-hydroxyethylammonium propionate, [E2HEA][Pr], over extended range of temperature and pressure. To the best of the authors' knowledge, the density and the speed of sound for [E2HEA][Pr] is here reported for the first time.

The IL volumetric behavior is described here in terms of the Goharshadi–Morsali–Abbaspour equation of state (GMA EoS), which has been developed and found to be valid for polar, non-polar, and H-bonded fluids [24]. From GMA EoS, the thermal expansivity and isothermal compressibility were evaluated. From experimental density and speed of sound data, isentropic compressibilities were calculated and molar compressibilities values evaluated and discussed using speed of sound and isothermal compressibilities.

2. Experimental

2.1. Materials

The *N*-ethyl-2-hydroxyethylammonium propionate was synthesized from stoichiometric quantities of the N-ethylethanolamine and propanoic acid using the methodology described in detail by Talavera-Prieto et al. [21]. In order to reduce to negligible values both water and volatile compounds, vacuum (1 Pa), stirring and moderate temperature (303 K) were applied prior to the measurements for a period of at least 48 h. The PIL purity was further checked by ^{1}H NMR and ^{13}C NMR using dimethylsulfoxide (DMSO) as a solvent (see Figs. S1 and S2 in Supporting Information). The NMR spectra, and the peak integration, show clearly the correct stoichiometry and the high purity of the synthesized compound. Note that only the ^{1}H NMR is quantitative and thus, useful to evaluate the compound's purity; the purity was found to be greater than 98% with water content lower than 100 ppm. The IL water content was determined with a Metrohm 831 Karl Fisher coulometer (using the Hydranal–Coulomat AG from Riedel-de Haens as analyte).

The chemical structure, compound description, CAS number, water mass fraction content, mass fraction purity and supplier, of the IL and calibration liquids are reported in Table 1. The water used was HPLC (high performance Liquid Chromatography/Scharlau) (indicated by its electrical conductivity of 1μS/cm). The toluene used was of analytical quality, also to a high purity, 0.9999 (w/w).

2.2. Density measurements

An Anton Paar DMA 60 digital vibrating-tube densimeter, with a DMA 512P measuring cell, was used for measurements of densities, ρ, within the temperature range of 298.15–343.15 K and pressures ranging from (0.1 to 35.0) MPa. The installation of the DMA measurement system including the peripheral equipment was described in detail in a previous work [21]. The temperature inside the vibrating-tube cell was measured with a Pt100 with an uncertainty of 0.02 K and it was regulated by an external circulating fluid Julabo P-5 thermostatic bath with silicone oil. The Pt100 was previously calibrated in the 273.15–373.15 K temperature range against a platinum resistance thermometer ERTCOEutechnics High Precision Digital Thermometer certified in the ITS90. The required pressure was generated and controlled with a Pressure Generator model 50-6-15, High Pressure Co. Pressure was measured with a pressure transducer (Wika Transmitter S-10) with a maximum uncertainty of 0.03 MPa. Water and toluene were used as reference fluids to fit the calibration equation proposed by Lampreia and Nieto de Castro [25]. The combined standard uncertainty of the density measurements was found to be $u_c(\rho)$ = 0.45 kg·m^{-3}, which was estimated taking into account the influence of uncertainties associated with the calibration equation, temperature, period of oscillations (six-digit frequency counter), viscosity, and density data of calibrating fluids.

2.3. Speed of sound measurements

The speed of sound, u, was measured along six isotherms over a temperature range from 303.15 to 353.15 K and for pressures up to 20 MPa by using a stainless steel cell designed for liquid measurements, which is fully described in [26]. The instrumentation and the speed of sound measurement procedure used in this work are reported in [15] and summarized here.

Two 5 MHz ultrasonic transducers in through transmission mode are mounted in cavities drilled on a stainless steel block. The ultrasound wave propagating between the transmitter and receiver is collected by a NI-PCI data acquisition board and saved in a computer for processing. A developed Labview program allows an easy wave propagation time calculation, in the liquid, which is obtained subtracting the time that the acoustical wave takes to

Table 1
Chemical structure, compound description, CAS Number, molecular weight, water mass fraction content, mass fraction purity and supplier of the studied compounds.

Compound	Chemical structure
N-Ethylethanolamine (CAS: 110-73-6; Mw = 89.14 g·mol^{-1}; wt% ≥98%[a]) acquired from Sigma-Aldrich	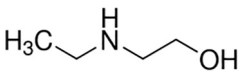
Propanoic Acid (CAS:79-09-4; Mw = 74.08 g·mol^{-1}; wt% ≥98%[a]) acquired from Sigma-Aldrich	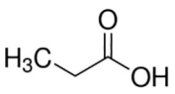
Water (CAS:7732-18-5; Mw = 18.02 g·mol^{-1}; wt% ≥98%[a]) obtained from Milli-Q	
Toluene (CAS:108–88-3; Mw = 92.14 g·mol^{-1}; wt% ≥99.999%[a]) acquired from Fisher Scientific	
N-ethyl-2-hydroxyethylammonium propionate ([E2HEA][Pr]) (Mw = 163.22 g·mol^{-1}; H_2O wt < 100 ppm; wt% ≥98%[b])	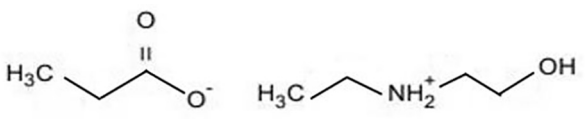

[a] as reported by the supplier.
[b] after moderate temperature and vacuum procedure.

travel between the emitter and receiver from the propagation time in the cell steel walls.

The system temperature was controlled by means of a flexible silicone resistance cable wrapped around the cell, using an electronic thermostat (Red Line Series RD31) whose temperature probe is inserted in the resistance coil. The experimental setup was placed in a thermal insulation glove box, to avoid heat losses, and is able to maintain the temperature within *ca.* ±0.1 K. The temperature was measured using an external digital thermometer by isothermal Technology (ISOTECH TTI-10), with a precision of 0.01 K, placed directly in a cavity of the cell and close to the sample. The pressure was measured using a manometer by Keller (Mano 2000 LEO 2), with an accuracy of ±0.02 MPa. The cell was calibrated by measuring the speed of sound in water [27] and toluene [27], for the overall temperature and pressure ranges T = (298.15–348.15) K, and p = (0.1–20) MPa, using a total of 156 data points. The calibration equation from Gomes de Azevedo and coworkers' [28], already reported by the authors in a previous work [15], was used. Taking in consideration the temperature, pressure, and the calibrating fluids speed of sound uncertainties, the combined standard uncertainty in the reported speed of sound values was estimated to be $u_c(u)$ = 1.6 m.s^{-1}.

3. Results and discission

3.1. 3.1. High-pressure density

The density of [E2HEA][Pr] was measured from 298.15 K to 343.15 K in 10 K steps and for pressures up to 35.0 MPa. The experimental densities are presented in Table 2 and in Fig. 1(a) for the six measured isotherms. It can be seen a slight non-linear behaviour of the density versus the pressure in each isotherm. It can be stated that the density values increase for increasing pressures and decreasing temperatures, with a maximum of 1064.6 kg·m^{-3} obtained at 298.15 K and 35 MPa. Fig. 1(b) presents the experimental densities for the isobars (0.1, 10, 20 and 30) MPa. It can be seen also a slight non-linear behaviour of the density versus temperature on each isobaric line, which undergo some spreading as the temperature increases. At low pressures the density values are visibly lower than for the higher pressures and also decrease as the temperature increases, as expected.

The Goharshadi–Morsali–Abbaspour equation of state (GMA EoS) is [24]:

$$B(T)\rho_m^5 + A(T)\rho_m^4 + \rho_m - 2p/RT = 0 \quad (1)$$

where ρ_m is the molar density and $A(T)$ and $B(T)$ are temperature dependent parameters given by the equations [24]:

$$A(T) = A_0 - \frac{2A_1}{RT} + \frac{2A_2 \ln T}{R} \quad (2)$$

$$B(T) = B_0 - \frac{2B_1}{RT} + \frac{2B_2 \ln T}{R} \quad (3)$$

where A_0-A_2 and B_0-B_2 are fitting parameters, and R is the gas constant. Eq. (1) can be written in the linear form:

$$(2z-1)V_m^3 = A(T) + B(T)\,\rho_m \quad (4)$$

where z and V_m are the compressibility factor and the molar volume, respectively. The parameters A_0-A_2 and B_0-B_2 were calculated by least squares fitting Eq. (4) to density data of Table 2 and are given in Table 3 along with the the absolute average relative deviation ($\%AARD_\rho$), the average absolute deviation (AAD_ρ), and the standard deviation for density (σ_ρ) of the results defined as:

$$\%AARD_\rho = \frac{100}{N} \times \sum_{i=1}^{N} \left| \frac{\rho_{calc} - \rho}{\rho} \right| \quad (5)$$

$$AAD_\rho = \frac{1}{N} \times \sum_{i=1}^{N} |\rho_{calc} - \rho| \quad (6)$$

$$\sigma_\rho = \left[\sum_{i=1}^{N_p} (\rho_{cal} - \rho)_i^2 / (N-k) \right]^{1/2} \quad (7)$$

where, ρ_{cal} is the calculated density from GMA EoS, and ρ is the experimental one, for the measurement i, respectively, with k (= 6) the number of fitted parameters. The statistical indicators allowed to conclude that GMA EoS gives an excellent pVT data correlation with $AARD$ = 0.03% and standard deviation of 0.4 kg·m^{-3}, which is similar to combined uncertainty. Furthermore, it was verified that absolute differences in density $|\rho_{calc}$-$\rho|$ are usually lower than 0.7 kg·m^{-3} (AAD_ρ = 0.3 kg·m^{-3}).

In Fig. 1 the experimental ρ values are compared with those obtained from Eq. (4) for the studied isotherms. The excellent agreement between experimental and calculated values from correlation with GMA EoS can be observed. From Eq. (4), it can be concluded that under isothermal conditions, the quantity $(2z-1)V_m^3$, as a function of molar density, will have linear behavior. In Fig. 2, the term $(2z-1)V_m^3$ is plotted against molar density for isothermal conditions. The excellent agreement between experimental data

Table 2
Experimental density data (ρ) for [E2HEA][Pr] as a function of temperature (T) and pressure (p).[a]

p	T	ρ	T	ρ	T	ρ
MPa	K	Kg·m^{-3}	K	kg·m^{-3}	K	kg·m^{-3}
0.1	298.16	1051.9	313.14	1035.6	333.16	1011.9
10.0	298.15	1057.0	313.09	1041.8	333.14	1018.0
15.0	298.14	1058.3	313.11	1043.2	333.15	1021.0
20.0	298.16	1059.9	313.09	1045.6	333.16	1023.7
25.0	298.15	1061.8	313.07	1047.8	333.16	1026.2
30.0	298.14	1063.5	313.07	1049.6	333.15	1028.8
35.0	298.15	1064.6	313.07	1051.4	333.15	1031.3
0.1	303.16	1046.7	323.15	1024.4	343.17	998.8
10.0	303.15	1052.1	323.16	1030.5	343.17	1004.6
15.0	303.15	1053.4	323.15	1032.6	343.14	1008.7
20.0	303.14	1055.6	323.15	1035.2	343.21	1011.2
25.0	303.14	1057.4	323.15	1037.2	343.14	1014.3
30.0	303.12	1059.2	323.15	1039.3	343.17	1017.4
35.0	303.08	1060.7	323.15	1041.5	343.19	1020.1

[a] Standard uncertainties are u (T) = 0.02 K, u (p) = 0.03 MPa and u_c (ρ) = 0.45 kg·m^{-3}.

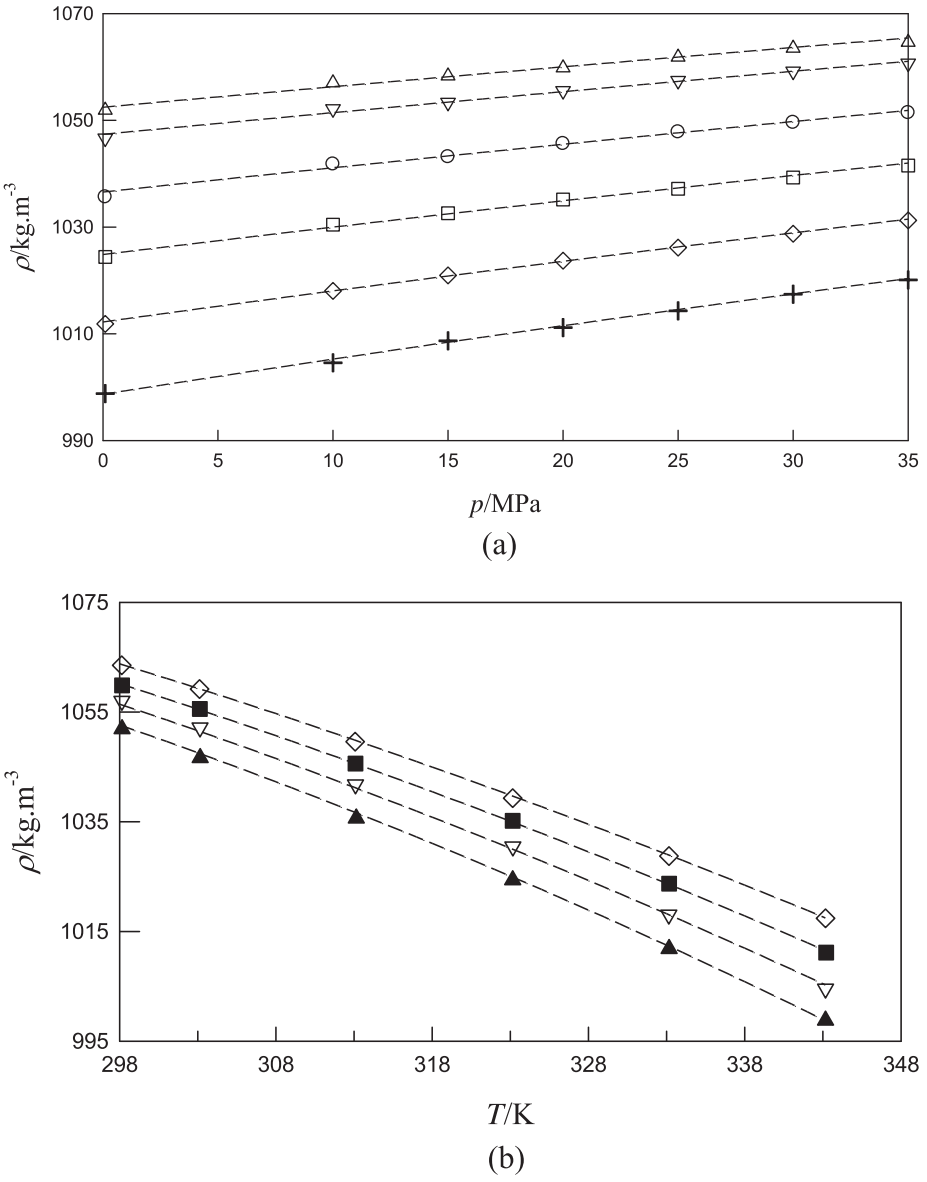

Fig. 1. Experimental density (ρ) as function of pressure for the isotherms (a) and as function of temperature for some isobars (b).The dashed lines represent the GMA EoS description for [E2HEA][Pr]: (a):Δ, 298.15 K; ∇, 303.15 K; ○, 313.15 K; □, 323.15 K; ◇, 333.15 K; +, 343.15 K. For (b) ▲, 0.1 MPa; ∇, 10 MPa; ■, 20 MPa; ◇, 30 MPa.

Table 3
Parameters A_0-A_2, and B_0-B_2 of Eqs. (2) and (3), temperature and pressure ranges (T_{min}, T_{max}, p_{min}, p_{max}), standard deviation (σ) coefficient of determination (r^2) number of data points (N), and standard deviation on density (σ_ρ).

M/g.mol^{-1}	163.21	p_{min}/MPa	0.10
A_0 /dm^9·mol^{-3}	48.4435	p_{max}/MPa	35.0
A_1 /MPa·dm^{12}·mol^{-4}	13.8975	σ/dm^9·mol^{-3}	4×10^{-4}
A_2 /MPa·dm^{12}·mol^{-4}· K^{-1}	−0.0280971	r^2	0.994
B_0 /dm^{12}.mol^{-4}	−6.70459	σ_ρ/kg·m^{-3}	0.42
B_1 /MPa·dm^{15}·mol^{-5}	−1.94734	N	42
B_2 /MPa·dm^{15}·mol^{-5}· K^{-1}	0.00388967	$\%AARD_\rho$	0.03
T_{min}/K	298.14	AAD_ρ/kg·m^{-3}	0.3
T_{max} /K	343.19		

and analytical behavior of GMA EoS, as well as the linear behavior are observed.

Fig. 3 compares the calculated densities from Eq. (4) with experimental data in the studied ranges of temperatures and pressures. In the calculations, the relative percentage deviation ($\%RD_\rho$), of the results is:

$$\%RD_\rho = 100 \times \frac{\rho_{calc} - \rho}{\rho} \quad (8)$$

As can be seen, the relative deviations are very small, ranging within ±0.05%.

In a previous publication [15] the density of 2-hydroxyethylammonium propionate was evaluated as function of pressure and temperature. As one would expect, the substitution of one of the cation's hidrogens, on the 2-hydroxyethylammonium propionate IL, by a ethyl group, leads to a decrease on the density (in average 67 kg.m^{-3}) and an increase of of 3.49×10^{-5} m^3.mol^{-1}, in average, on the molar volume; increase that, due to the molar volumes additive characteristic, corresponds to the molar volume of the ethyl group.

3.2. High-pressure speed of sound

The speed of sound measured along isothermal steps of 10 K in the temperature range T = (303.15–353.15) K for pressures up to 20 MPa are reported in Table 4 and plotted in Fig. 4.

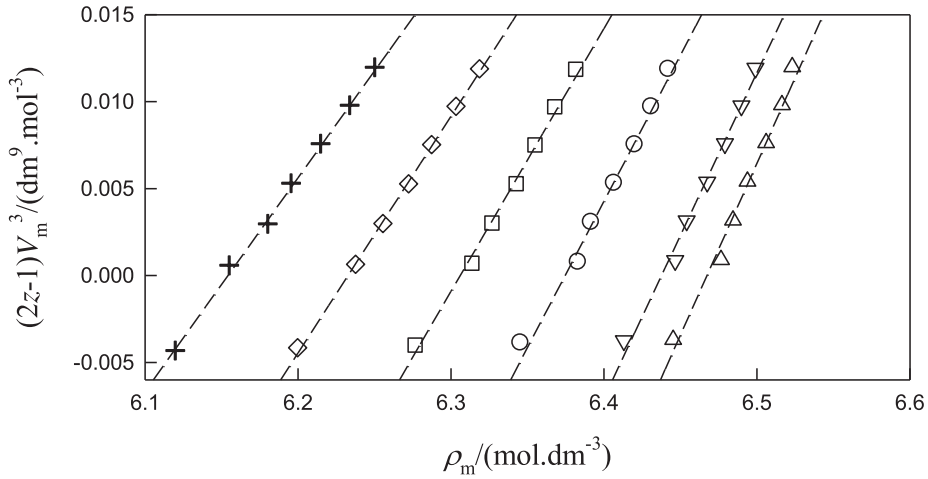

Fig. 2. Isotherms of $(2z\text{-}1)V_m^3$ versus the molar density (ρ_m) for [E2HEA][Pr] calculated from GMA EoS. Experimental data: Δ, 298.15 K; ▽, 303.13 K; ○, 313.09 K; □, 323.15 K; ◇, 333.15 K; +, 343.17 K. The lines represent the fit with GMA EoS.

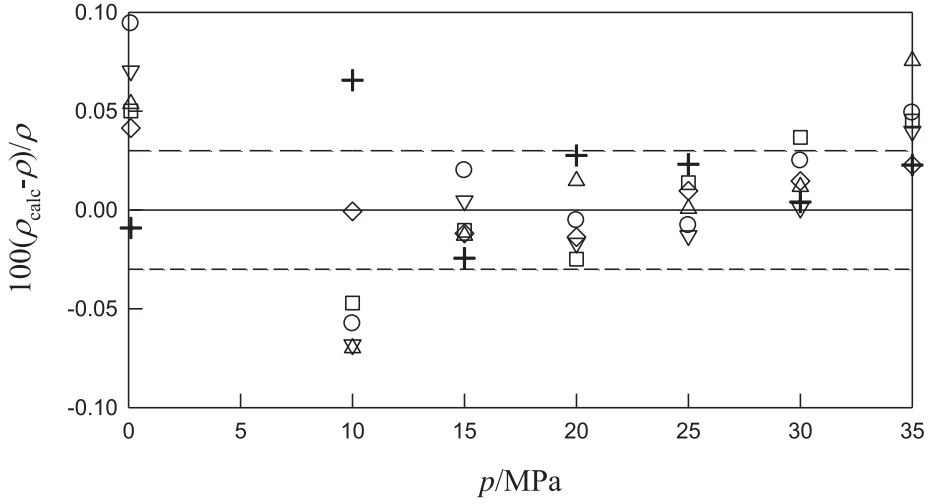

Fig. 3. Relative density deviations between the experimental density data (ρ) and those calculated by using the GMA EoS (ρ_{cal}) for [E2HEA][Pr]. Δ, 298.15 K; ▽, 303.15 K; ○, 313.15 K; □, 323.15 K; ◇, 333.15 K; +, 343.15 K. Dashed lines correspond to *AARD* = ±0.03%.

Table 4
Experimental values of speed of sound (u) for [E2HEA][Pr] as a function of temperature (T) and pressure (p).[a]

p/MPa	u (m·s^{-1}) at T(K)					
	303.15	313.15	323.15	333.15	343.15	353.15
0.1	1566.6	1535.6	1504.9	1485.5[a]	1450.5	1416.0
1.0	1570.6	1539.4	1508.6	1489.2[a]	1454.2	1419.9
2.0	1574.6	1543.3	1512.4	1494.2[a]	1458.0	1423.8
3.0	1578.7	1547.2	1517.3	1497.9[a]	1461.8	1428.9
4.0	1582.8	1552.4	1522.4	1500.5[a]	1466.7	1434.0
5.0	1586.9	1555.0	1527.4	1503.0	1470.5	1438.0
6.0	1589.6	1560.3	1531.2	1508.0	1474.3	1443.1
7.0	1592.4	1564.2	1535.0	1511.8	1478.1	1447.0
8.0	1595.1	1568.2	1538.9	1514.4	1481.9	1451.0
9.0	1599.3	1572.2	1542.8	1519.4	1485.7	1456.1
10.0	1603.5	1576.2	1546.6	1523.2	1489.5	1460.0
11.0	1607.7	1578.9	1550.5	1525.8	1493.3	1465.1
12.0	1611.9	1583.0	1555.7	1530.9	1497.2	1469.0
13.0	1616.1	1587.1	1559.7	1533.5	1501.0	1471.8
14.0	1620.3	1591.1	1563.6	1536.1	1504.8	1476.9
15.0	1623.2	1595.3	1566.3	1540.0	1507.4	1480.8
16.0	1627.4	1599.4	1570.3	1542.6	1511.2	1484.7
17.0	1631.7	1603.5	1572.9	1546.5	1516.3	1488.6
18.0	1634.6	1607.7	1575.6	1550.4	1520.1	1492.5
19.0	1637.5	1610.5	1579.6	1553.0	1524.0	1496.4
20.0	1640.4	1614.7	1583.7	1555.6	1526.6	1500.2

[a] The standard uncertainties u are $u(T)$ = 0.05 K, $u(p)$ = 0.02 MPa and $u_c(u)$ = 1.6 m·s^{-1}. At 333.15 K the uncertainties will be higher than 1.6 m·s^{-1} (at decreasing pressures from 5.0 to 0.1 MPa the uncertainty increase from *c. a.* 2 m·s^{-1} to 7 m·s^{-1}).

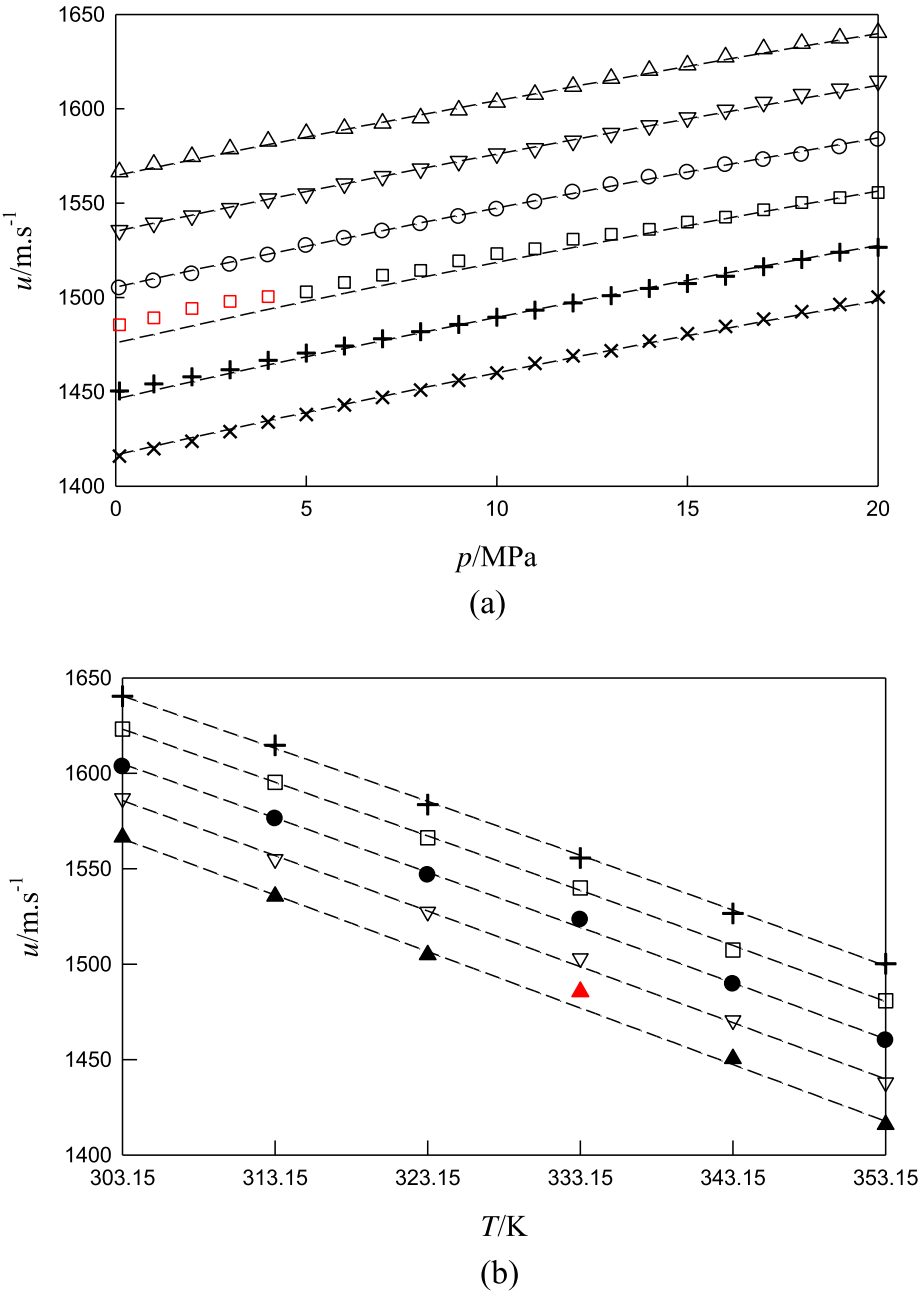

Fig. 4. Comparison between experimental speed of sound values (u) and those obtained by Eq. (9) for [E2HEA][Pr]: (a) versus the pressure at several temperatures, and (b) versus the temperature at several pressures. For (a): Δ, 303.15 K; ▽, 313.15 K; ○, 323.15 K; □, 333.15 K; +, 343.15 K; ×, 353.15 K. For (b) ▲, 0.1 MPa; ▽, 5 MPa; ●, 10 MPa; □, 15 MPa; +, 20 MPa. Red symbols represent data excluded from the fit with Eq. (9) represented by dashed lines. (For interpretation of the references to colour in this figure legend, the reader is referred to the web version of this article.)

Fom this figure it can be observed that some few measurements made at 333.15 K and for lower pressures especially bellow 5 MPa show unexpected uncertainties higher than 1.6 m.s^{-1}, the mentioned combined uncertainty. We found no plausible explanation for this anomalous behavior. The most important variables such as temperature, pressure always followed a normal control procedure during all the experiments and no anomaly was detected. Taking into account the large number of measurements made for the speed of sound, we chose to report these anomalous measurements by drawing attention to this fact. It should be mentioned that these measures were excluded from the correlation of data as explained below.

The speed of sound data, pressure and temperature were correlated by the equation:

$$p - p_0 = \sum_{i=1}^{3} \sum_{j=0}^{2} a_{ij} (u - u_0)^i T^j \tag{9}$$

suggested by Sun et al. [29]. The a_{ij} are the fitting parameters determined by least squares fitting of Eq. (9), u is the sound speed at $p > 0.1$ MPa, and u_0 is the speed of sound at $p = 0.1$ MPa. The speed of sound measured at atmospheric pressure was expressed as a parabolic function of temperature in the range (298.15–343.15) K:

$$u_0/\mathrm{m \cdot s^{-1}} = 2442.672 - 2.8341\,T - 1.9372 \cdot 10^{-4} T^2 \tag{10}$$

with a coefficient of determination of 0.999 and a standard deviation of 2.9 $m{\cdot}s^{-1}$. The coefficients a_{ij} and the the usual statistical indicators are presented in Table 5.

In Fig. 4(a), the experimental speed of sound values u, are compared with those calculated from Eq. (9) as function of pressure, for the six measured isotherms. It should be highlighted the difference of about 240 $m{\cdot}s^{-1}$ between the maximum (at 303.15 K and 20 MPa) and the minimum (at 353.15 K and 0.1 MPa) values for the speed of sound. For the 333.15 K isotherm and for pressures lower than 5 MPa appreciable deviations between for the Sun equation and experimental data are observed. The experimental values display positive deviations relative to the expected ones by 5 $m.s^{-1}$ or more and thus higher uncertainties than the reported standard uncertainty of 1.6 $m.s^{-1}$. The uncertainty for these experimental data was estimated from distribution of errors resulting by comparing experimental data with attached uncertainties (u_c = 1.6 $m{\cdot}s^{-1}$) with those fitted with Eq. (9) with corresponding uncertainties 1.8 $m{\cdot}s^{-1}$. At decreasing pressures from 5 MPa to 0.1 MPa the uncertainty should increase from 2 $m{\cdot}s^{-1}$ to 7 $m{\cdot}s^{-1}$. These experimental data were excluded from the fit with Eq. (9). In Fig. 4(b) the experimental speed of sound values are compared with those obtained with Eq. (9) versus the temperature, for the isobars (0.1, 5, 10, 15 and 20) MPa. As can be observed, the speed of sound has essentially a linear isobaric behavior, which value decreases as temperature increases.

As depicted in Fig. 5, where the %*RD*s are represented, it can be concluded that Eq. (9) gives a reliable correlation of the speed of sound for the studied ranges of temperatures and pressures with $\%AARD_u$ = 0.08% and the standard deviation σ_u = 1.8 $m{\cdot}s^{-1}$ (see Table 5). It was verified that about 79% of the values present deviations (u-u_{cal}) lower than σ_u: the maximum deviation obtained was (u-u_{cal}) = 5.8 $m{\cdot}s^{-1}$ at the coordinates T = 333.15, p = 6 MPa; the minimum deviation was 0.007 $m{\cdot}s^{-1}$ at T = 313.15 K, p = 7 MPa. Also, from Fig. 5, it is observed that the deviations are small, usually in the range of ±0.1% (about 1.6 $m{\cdot}s^{-1}$, corresponding to 76% of values). At atmospheric pressure, the *RD*% are within ±0.1%.

Table 5
Coefficients of Eq. (9), standard deviation (σ_u) coefficient of determination (r^2) number of data points (Np) and average absolute relative deviation, %*AARD*.

a_{10} / MPa·m·s^{-1}	1.27061
a_{11} / MPa·m·s^{-1}3 K^{-1}	−5.92117310^{-4}
a_{12} / MPa·m·s^{-1}3 K^{-2}	8.28908 × 10^{-6}
a_{20} / MPa·m^2·s^{-2}	3.83306 × 10^{-4}
r^2	0.995
$\sigma_{\Delta p}$/MPa	0.41
σ_u/m·s^{-1}	1.8
$\%AARD_u$	0.08
AAD/m·s^{-1}	1.3
N_p	121

3.3. Density and speed of sound derived properties

The thermal expansivity, $\alpha_p = -(1/\rho)(\partial\rho/\partial T)_p$, and isothermal compressibility $k_T = (1/\rho)(\partial\rho/\partial p)_T$, can be derived from the GMA equation of state as follows [30]:

$$\alpha_p = \frac{(2B_1 + 2B_2T)\rho_m^5 + (2A_1 + 2A_2T)\rho_m^4 + 2p}{5\rho_m^5\left(RT^2B_0 - 2B_1T + 2B_2T^2\ln T\right) + 4\rho_m^4\left(RT^2A_0 - 2A_1T + 2A_2T^2\ln T\right) + RT^2\rho_m} \quad (11)$$

$$k_T = \frac{2}{\rho_m RT + 5\rho_m^5(RTB_0 - 2B_1 + 2B_2T\ln T) + 4\rho_m^4(RTA_0 - 2A_1 + 2A_2T\ln T)} \quad (12)$$

The density variations over isothermal or isobaric paths are usually smooth functions of temperature and pressure. However, the mechanical coefficients are quite sensitive to subtle changes in the density. The calculated α_p and k_T, from GMA EoS, are presented in Table 6. Fig. 6 shows the behavior of α_p as function of temperature and pressure. The expected behavior is observed, *i.e.* α_p decreases with the increase of pressure, at isothermal conditions and increases with the temperature, at fixed pressures.

The isothermal compressibility is represented in Fig. 7 as function of temperature and pressure. As commonly observed, k_T increases with temperature at isobaric conditions and decreases with pressure for fixed temperatures.

The values of α_p and k_T for [E2HEA][Pr] are only slightly higher than those calculated, with the same EoS for [2HEA][Pr] reported in a previous work [15].

The measured densities and sound speeds were combined through Newton-Laplace equation to calculate the isentropic compressibility, k_s:

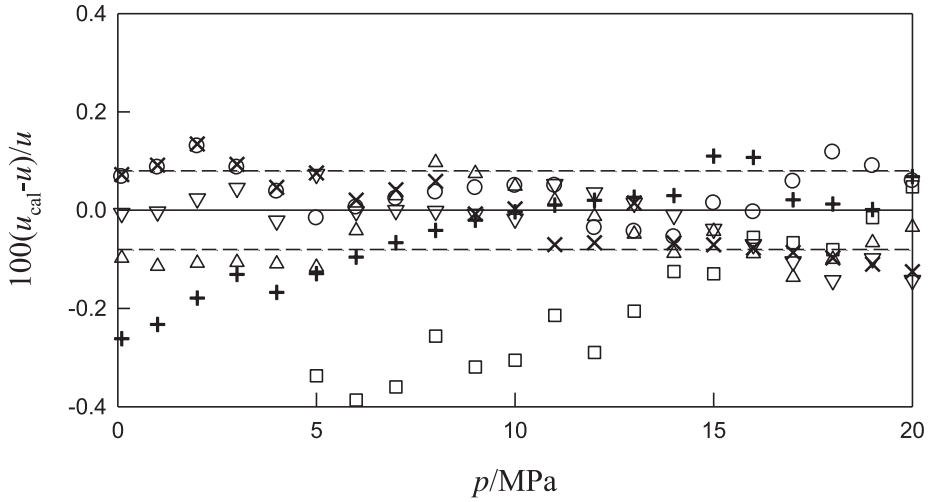

Fig. 5. Relative deviations of the speed of sound between experimental (u) and calculated values using Eq. (9) (u_{cal}). Δ, 303.15 K; ▽, 313.15 K; ○, 323.15 K; □, 333.15 K; +, 343.15 K; ×, 353.15 K. The dashed lines represent the limits for $\%AARD_u$ = ±0.08% (see Table 5).

Table 6
Thermal expansivity (α_p) and isothermal compressibility (k_T) calculated from GMA EoS.[a]

T/K	p/MPa	α_px10^4/K^{-1}	k_T/GPa^{-1}	T/K	p/MPa	α_px10^4/K^{-1}	k_T/GPa^{-1}
298.16	0.1	9.460	0.369	323.15	0.1	11.860	0.509
298.15	10.0	9.030	0.357	323.16	10.0	11.210	0.487
298.14	15.0	8.820	0.351	323.15	15.0	10.890	0.476
298.16	20.0	8.610	0.346	323.15	20.0	10.600	0.466
298.15	25.0	8.420	0.341	323.15	25.0	10.310	0.457
298.14	30.0	8.220	0.336	323.15	30.0	10.040	0.448
298.15	35.0	8.040	0.331	323.15	35.0	9.780	0.439
303.16	0.1	9.910	0.392	333.16	0.1	12.930	0.583
303.15	10.0	9.440	0.379	333.14	10.0	12.150	0.554
303.15	15.0	9.210	0.373	333.15	15.0	11.790	0.541
303.14	20.0	8.990	0.367	333.16	20.0	11.440	0.529
303.14	25.0	8.780	0.361	333.16	25.0	11.110	0.516
303.12	30.0	8.570	0.355	333.15	30.0	10.790	0.505
303.08	35.0	8.370	0.349	333.15	35.0	10.490	0.494
313.14	0.1	10.850	0.445	343.17	0.1	14.030	0.673
313.09	10.0	10.290	0.428	343.17	10.0	13.110	0.635
313.11	15.0	10.030	0.420	343.14	15.0	12.680	0.617
313.09	20.0	9.770	0.412	343.21	20.0	12.280	0.601
313.07	25.0	9.520	0.405	343.14	25.0	11.890	0.585
313.07	30.0	9.290	0.398	343.17	30.0	11.530	0.571
313.07	35.0	9.060	0.391	343.19	35.0	11.190	0.557

[a] Using the propagation law of errors the estimated maximum uncertainties u are $u(\alpha_p) = 2 \times 10^{-7}$ K^{-1} and $u(k_T) = 3 \times 10^{-3}$ GPa^{-1}.

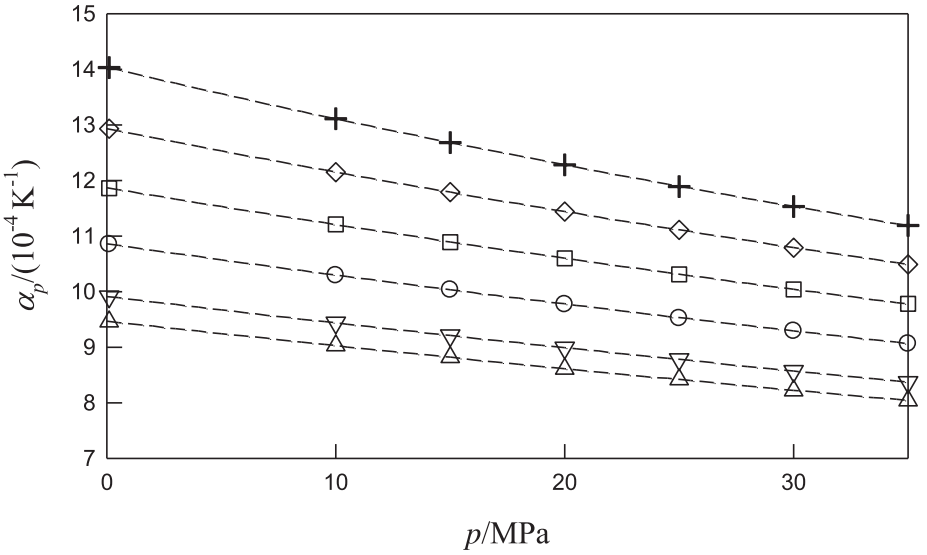

Fig. 6. Thermal expansivity of [E2HEA][Pr] as a function of pressure and temperature determined through GMA EoS: Δ, 298.15 K; ∇, 303.15 K; ○, 313.15 K; □, 323.15 K; ◇, 333.15 K; +, 343.15 K. The dashed lines are guides to the eyes.

$$k_S = \frac{1}{\rho\, u^2} \tag{13}$$

The k_S values as a function of pressure and temperature are presented in Table 7 and Fig. 8. From Fig. 8, it can be observed that k_S presents the common behavior observed for ionic liquids, with T and p that in turn is related to the corresponding behavior of density and speed of sound: k_S increases with temperature at isobaric conditions and decreases with pressure at isothermal conditions. At 298.15 K and 0.1 MPa, $k_S = 3.81 \times 10^{-10}$ Pa^{-1} can be calculated from density and speed of sound obtained from GMA EoS and Sun equation, respectively. This value can be compared with $k_S = 3.62 \times 10^{-10}$ Pa^{-1} obtained previously by the authors for 2-hydroxyethylammonium propionate [2HEA][Pr] [15] and thus, an increment of about 5% in k_S will be due to the addition of an ethyl group to 2-hydroxyethylammonium cation.

An important parameter in the study of liquid state is the molar compressibility, also called Wada's constant, [31] defined by:

$$k_\mathrm{m} = \frac{M}{\rho}\, k_S^{-1/7} \tag{14}$$

The molar compressibility of [E2HEA][Pr] was calculated from experimental densities and speeds of sound in the ranges $T = (303.15–343.15)$ K and $p = (0.1–20)$ MPa and is presented in Table 8. It can be observed that k_m is almost constant as function of temperature and pressure. As the molar compressibility presents a small temperature and pressure dependency, the mean value $<k_\mathrm{m}>$ was determined as:

$$< k_\mathrm{m} >= (1/N) \sum_i^N (k_\mathrm{m})_i \tag{15}$$

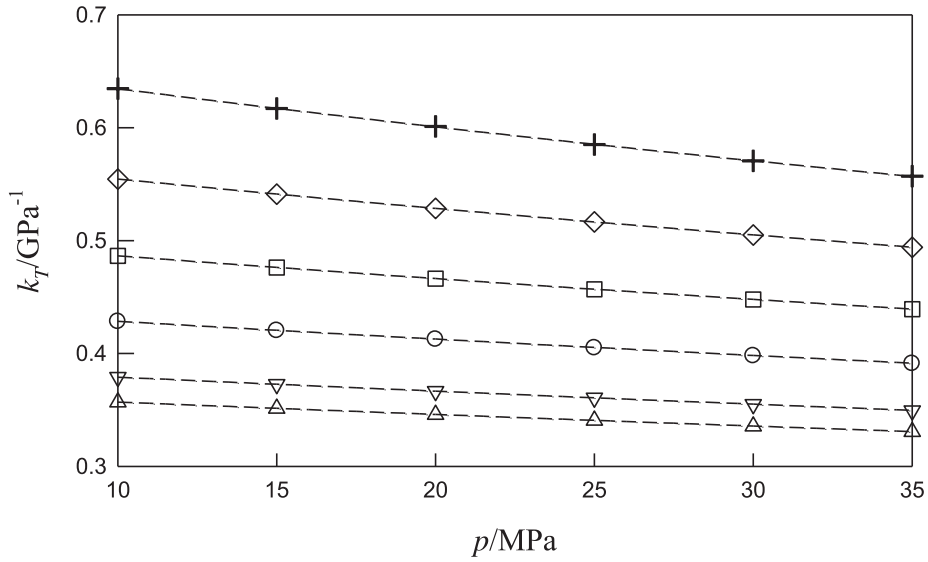

Fig 7. Isothermal compressibility of [E2HEA][Pr] as function of pressure and temperature from GMA EoS. Δ, 298.15 K; ▽, 303.15 K; ○, 313.15 K; □, 323.15 K; ◇, 333.15 K; +, 343.15 K. The dashed lines are guides for the eyes.

Table 7
Experimental isentropic compressibility (k_S) as function of temperature and pressure.[a]

p/MPa	$10^{10}\cdot k_S$/Pa^{-1}				
	303.15 K	313.15 K	323.15 K	333.15 K	343.15 K
0.1	3.89	4.09	4.31	4.48	4.76
10.0	3.70	3.86	4.06	4.23	4.49
15.0	3.60	3.77	3.95	4.13	4.36
20.0	3.52	3.67	3.85	4.04	4.24

[a] The estimated maximum uncertainty u is $u(k_S) = 9 \times 10^{-13}$ Pa^{-1} from the propagation law of errors.

over the range of pressure variation ($<k_m>, p)_T$ for each isotherm and over the temperature variation ($<k_m>, T)_p$ at each pressure. The corresponding standard deviation from the mean values for each isotherm or isobar was calculated as:

$$\sigma_{km} = \left[\sum_{i=1}^{N} (k_m - < k_m >)_i^2 / N\right]^{1/2} \quad (16)$$

From the values ($<k_m>, p)_T$ and ($<k_m>, T)_p$ the overall mean values were calculated giving $< k_m> = (3.484 \pm 0.022) \times 10^{-3}$/(m·mol^{-1}. Pa$^{1/7}$) and $< k_m> = (3.484 \pm 0.007) \times 10^{-3}$ /(m·mol^{-1}. Pa$^{1/7}$), respectively. The value $<k_m> = 3.484 \times 10^{-3}$ (m·mol^{-1}. Pa$^{1/7}$) is in sequence with $<k_m> = 2.731 \times 10^{-3}$/(m·mol^{-1}. Pa$^{1/7}$) and $<k_m> = 3.138 \times 10^{-3}$/(m·mol^{-1}. Pa$^{1/7}$) obtained previously by the authors for 2-hydroxyethylammonium propionate [2HEA][Pr] [15] and N-methyl-2-hydroxyethylammonium propionate [m2HEA][Pr] [19]. Thus, the influence of adding a –CH_2– group in the cation is an increase of about 0.35×10^{-3} m^{3}3mol^{-1}. Pa$^{1/7}$ (about 10%) in $<k_m>$. In this way, $<k_m>$ can be considered as an appropriate and useful parameter characteristic of the IL over a broad range of pressures and temperatures. For example, Eq. (14) can be solved for the speed of sound using Eq. (13) and assuming that $k_m = <k_m>$:

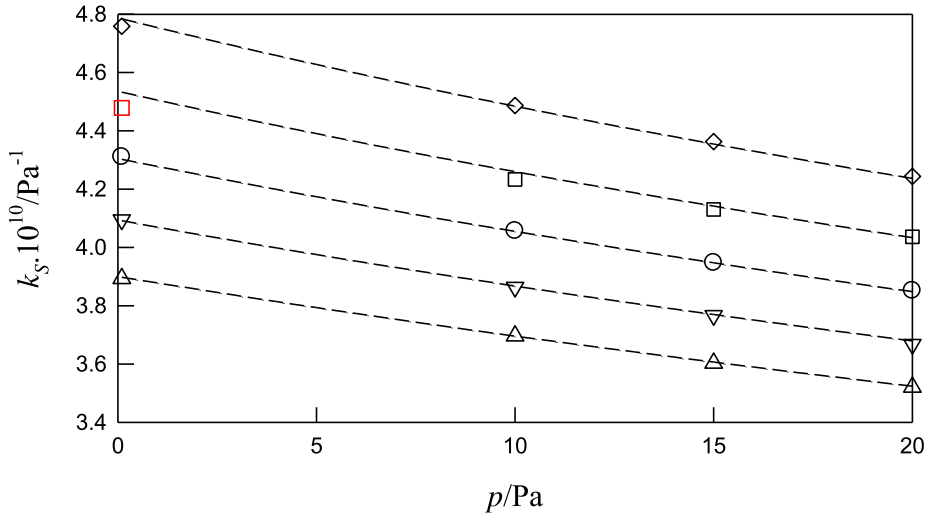

Fig. 8. Isentropic compressibility of [E2HEA][Pr] as function of temperature and pressure determined from GMA EoS: Δ, 303.15; ▽, 313.15 K; ○, 323.15 K; □, 333.15 K; ◇, 343.15 K. Dashed lines are guides to the eyes. Red square represents data excluded from Eq. (9) fit. (For interpretation of the references to colour in this figure legend, the reader is referred to the web version of this article.)

Table 8
Molar compressibility (k_m) of [E2HEA][Pr] as function of temperature and pressure. The mean molar compressibilities (<k_m>) taken over pressure or temperature ranges, and corresponding standard deviations are presented.

p/MPa	k_m 10^3/m^3.mol^{-1}. Pa$^{1/7}$					
	303.15 K	313.15 K	323.15 K	333.15 K	343.15 K	(<k_m>, T)$_p$ ± σ
0.1	3.445	3.457	3.469	3.493	3.508	3.474 ± 0.023
10.0	3.452	3.465	3.479	3.500	3.517	3.483 ± 0.023
15.0	3.461	3.473	3.485	3.502	3.517	3.488 ± 0.020
20.0	3.465	3.478	3.488	3.504	3.522	3.492 ± 0.020
(<k_m>, p)$_T$ ± σ	3.456 ± 0.008	3.468 ± 0.008	3.480 ± 0.007	3.500 ± 0.004	3.516 ± 0.005	3.484 ± 0.007[a] 3.484 ± 0.022[b]
Total < k_m>±σ	3.484 ± 0.023					

[a] <km> for (<k_m>, T)$_p$.
[b] <km> for (<k_m>, p)$_T$.

$$u = \left(\frac{< k_m >}{M}\right)^{7/2} \rho^3 \quad (17)$$

Thus, the speed of sound can be estimated at any desired temperature and pressure from density. For [E2HEA][Pr] the speed of sound can be predicted with *%AARD* = 2.0%.

4. Conclusions

Density and speed of sound were measured for *N*-ethyl-2-hydroxyethylammonium propionate for the first time. A total of 42 density points have been measured in the pressure range from atmospheric pressure to 35 MPa and along six isotherms within temperature interval (293.15–343.15) K using a vibrating tube densimeter. The experimental densities are very well correlated with the GMA EoS with an average absolute relative deviation of 0.03% corresponding to the average absolute deviation of 0.3 kg·m^{-3}. Comparing the results for density of *N*-ethyl-2-hydroxyethylammonium propionate with those for 2-hydroxyethylammonium propionate we concluded that substitution of one of the cation's hidrogens, on the 2-hydroxyethylammonium propionate IL, by a ethyl group, leads to a decrease on the density (in average 67 kg.m^{-3}) and an increase of 3.49×10^{-5} m^3.mol^{-1}, in average, on the molar volume, corresponding to the molar volume of the ethyl group.

By deriving the GMA EoS, thermal expansivity and isothermal compressibility were determined in the same p and T ranges. These properties behave as expected relative to temperature and pressure variations. A total of 126 speed of sound points are reported along six isotherms from 303.15 to 353.15 K and at pressures from the atmospheric up to 20 MPa. To accomplish these measurements, an acoustic cell and a *Labview* interface designed for signal acquisition and processing were used. The experimental (*upT*) speed of sound data is well correlated with a Sun type function with an average absolute relative deviation of 0.08% corresponding to the average absolute deviation of 1.3 m·s^{-1}. The density and speed of sound measurements were used to calculate the isentropic compressibilities by means of Laplace equation and also molar compressibilities. The molar compressibility is almost constant presenting a variation of only 2% over the pressure and temperature intervals of 0.1 MPa to 20 MPa and from 303 to 343 K. Based in previous studies we conclude that adding a –CH_2– group to the 2-hydroxyethylammonium cation an increase of about 0.35×10^{-3} m·mol^{-1}. Pa$^{1/7}$ (about 10%) in <k_m> results.

Acknowledgments

Part of this work was developed in the scope of the project CICECO-Aveiro Institute of Materials, POCI-01-0145-FEDER-007679 (ref. FCT UID/CTM/50011/ 2013), funded by FEDER through COMPETE2020 - Programa Operacional Competitividade e Internacionalização (POCI) and by national funds through FCT - Fundação para a Ciência e a Tecnologia. P. J. Carvalho acknowledges FCT for a contract under the Investigador FCT 2015, Contract IF/00758/2015.

Appendix A. Supplementary data

Supplementary data to this article can be found online at https://doi.org/10.1016/j.jct.2018.11.005.

References

[1] D.F. Kennedy, C.J. Drummond, Large aggregated ions found in some protic ionic liquids, J. Phys. Chem. B 113 (2009) 5690.
[2] J. Pernak, I. Goc, I. Mirska, Anti-microbial activities of protic ionic liquids with lactate anion, Green Chem. 6 (2004) 323–329.
[3] K. Yamamoto, H. Sakaguchi, H. Anai, T. Tanaka, K. Morimoto, K. Kichikawa, H. Uchida, Sclerotherapy for simple cysts with use of ethanolamine oleate: preliminary experience, Cardiovasc. Intervent. Radiol. 28 (2005) 751–755.
[4] M.G. Kiripolsky, More on ethanolamine oleate as a vascular sclerosant, Dermatol. Surg. 36 (2010) 1153–1154.
[5] R.V. Hangarge, D.V. Jarikote, M.S. Shingare, Knoevenagel condensation reactions in an ionic liquid, Green Chem. 4 (2002) 266–268.
[6] M.J. Earle, N.V. Plechkova, K.R. Seddon, Green synthesis of biodiesel using ionic liquids, Pure Appl. Chem. 81 (2009) 2045–2057.
[7] M.A.B.H. Susan, A. Noda, S. Mitsushima, M. Watanabe, Brønsted acid–base ionic liquids and their use as new materials for anhydrous proton conductors, Chem. Commun. 8 (2003) 938–939.
[8] S. Zhu, P.D.A. Pudney, M. Heppenstall-Butler, M.F. Butler, D. Ferdinando, M. Kirkland, Interaction of the acid soap of triethanolamine stearate and stearic acid with water, J. Phys. Chem. B 111 (2007) 1016–1024.
[9] J.C. Galvez-Ruiz, G. Holl, K. Karaghiosoff, T.M. Klapotke, K. Lohnwitz, P. Mayer, H. Noth, K. Polborn, C.J. Rohbogner, M. Suter, J.J. Weigand, Derivatives of 1,5-Diamino-1*H*-tetrazole: a new family of energetic heterocyclic-based salts, Inorg. Chem. 44 (2005) 4237–4253.
[10] K.A. Kurnia, C.D. Wilfred, T. Murugesan, Thermophysical properties of hydroxyl ammonium ionic liquids, J. Chem. Thermodyn. 41 (2009) 517–521.
[11] M. Iglesias, R. Gonzalez-Olmos, I. Cota, F. Medina, Brønsted ionic liquids: study of physico-chemical properties and catalytic activity in aldol condensations, J. Chem. Eng. Data 162 (2010) 802–808.
[12] X. Wang, C. Ohlin, Q.Lu.Z. Fei, J. Hu, P.J. Dyson, Cytotoxicity of ionic liquids and precursor compounds towards human cell line HeLa, Green Chem. 9 (9) (2007) 1191–1197.
[13] M.V.S. Oliveira, B.T. Vidal, C.M. Mel, R.C.M. de Miranda, C.M.F. Soares, J.A.P. Coutinho, S.P.M. Ventura, S. Mattedi, A.S. Lima, (Eco)toxicity and biodegradability of protic ionic liquids, Chemosphere 147 (2016) 460–466.
[14] K.A. Kurnia, M.M. Taib, M.I.A. Mutalib, Densities, refractive indices and excess molar volumes for binary mixtures of protic ionic liquids with methanol at T = 293.15 to 313.15 K, J. Mol. Liq. 159 (2011) 211–219.
[15] J.A. Sarabando, P.J.M. Magano, A.G.M. Ferreira, J.B. Santos, P.J. Carvalho, S. Mattedi d, I.M.A. Fonseca, Influence of temperature and pressure on the density and speed of sound of 2-hydroxyethylammonium propionate ionic liquid, J. Chem. Thermodyn. 122 (2018) 183–193.
[16] V.H. Alvarez, N. Dosil, R. Gonzalez-Cabaleiro, S. Mattedi, M. Martin-Pastor, M. Iglesias, J.M. Navaza, Bronsted ionic liquids for sustainable processes: synthesis and physical properties, J. Chem. Eng. Data 55 (2010) 625–632.
[17] A. Pinkert, K.L. Ang, K.N. Marsh, S. Pang, Density, viscosity and electrical conductivity of protic alkanolammonium ionic liquids, Phys. Chem. Chem. Phys. 13 (2011) 5136–5143.
[18] A. Kazakov, J.W. Magee, R.D. Chirico, V. Diky, C.D. Muzny, K. Kroenlein, M. Frenkel, NIST Standard Reference Database 147: NIST Ionic Liquids Database – (ILThermo)", Version 2.0, Gaithersburg, MD: National Institute of Standards

and Technology. Available at: http:// ilthermo.boulder.nist.gov. (Accessed November, 2017).
[19] V.H. Alvarez, S. Mattedi, M. Martin-Pastor, M. Aznar, M. Iglesias, Thermophysical properties of binary mixtures of {ionic liquid 2-hydroxy ethylammonium acetate + (water, methanol, or ethanol)}, J. Chem. Thermodyn. 43 (2011) 997–1010.
[20] I. Cota, R. Gonzalez-Olmos, M. Iglesias, F. Medina, New short aliphatic chain ionic liquids: synthesis, physical properties, and catalytic activity in aldol condensations, J. Phys. Chem. B 111 (2007) 12468–12477.
[21] N.M.C. Talavera-Prieto, A.G.M. Ferreira, P.N. Simões, P.J. Carvalho, S. Mattedi, J. A.P. Coutinho, Thermophysical characterization of N-methyl-2-hydroxyethylammonium carboxilate ionic liquids, J. Chem. Thermodyn. 68 (2014) 221–234.
[22] Y. Li, E.J.P. Figueiredo, M.J.S.F. Santos, J.B. Santos, N.M.C. Talavera-Prieto, P.J. Carvalho, A.G.M. Ferreira, S. Mattedi, Volumetric and acoustical properties of aqueous mixtures of N-methyl-2-hydroxyethylammonium propionate at T = (298.15 to 333.15) K, J. Chem. Thermodyn. 88 (2015) 44–60.
[23] Y. Li, E.J.P. Figueiredo, M.J.S.F. Santos, J.B. Santos, N.M.C. Talavera-Prieto, P.J. Carvalho, A.G.M. Ferreira, S. Mattedi, Volumetric and acoustical properties of aqueous mixtures of N-methyl-2-hydroxyethylammonium butyrate and N-methyl-2-hydroxyethylammonium pentanoate at T = (298.15 to 333.15) K, J. Chem. Thermodyn. 97 (2016) 191–205.
[24] E.K. Goharshadi, A. Morsali, M. Abbaspour, New regularities and an equation of state for liquids, Fluid Phase Equilib. 230 (2005) 170–175.
[25] I.M.S. Lampreia, C.A. Nieto De Castro, A new and reliable calibration method for vibrating tube densimeters over wide ranges of temperature and pressure, J. Chem. Thermodyn. 43 (2011) 537–545.
[26] A.G.M. Ferreira, J.B. Santos, M.J. Santos, A.T.G. Portugal, Speed of sound in pure fatty acid methyl esters and biodiesel fuels, Fuel 116 (2014) 242–254.
[27] Thermophysical Properties of Fluid Systems - the NIST WebBook. http://webook.nist.gov/chemistry/fluid (accessed February, 2016).
[28] R. Gomes de Azevedo, J. Szydlowski, P. Pires, J. Esperanca, H. Guedes, L. Rebelo, A novel non-intrusive microcell for sound-speed measurements in liquids. Speed of sound and thermodynamic properties of 2-propanone at pressures up to 160 MPa, J. Chem. Thermodyn. 36 (2004) 211–222.
[29] T.F. Sun, S.N. Biswas, N.J. Trappeniers, C.A. Ten Seldam, Acoustic and thermodynamic properties of methanol from 273 to 333 K and at Pressures to 280 MPa, J. Chem. Eng. Data 33 (1988) 395–398.
[30] E.K. Goharshadi, M. Moosavi, Thermodynamic properties of some ionic liquids using a simple equation of state, J. Mol. Liq. 142 (2008) 41–44.
[31] Y. Wada, On the relation between compressibility and molal volume of organic liquids, J. Phys. Soc. Jpn. 4 (1949) 280–283.

JCT 18-115